Displacement of miscible viscous fluids from thin gaps

N. N. Smirnov V. F. Nikitin Yu. G. Phylippov V. R. Dushin
ebifsun1@mech.math.msu.su

Abstract

The goal of the present study is to investigate numerically and experimentally the peculiarities of two-component viscous fluid flow in a thin plane channel, and to determine entrapment and flushing out one component by the other. Experiments on miscible displacement of fluids in Hele-Shaw cells were conducted under microgravity conditions. Extensive direct numerical simulations allowed to investigate the sensitivity of fluid flow to variation of values of the main governing parameters. Validation of the code was performed by comparing the results of model problems simulations with experiments.

1 Introduction

Viscous fluids flow in gaps and blocked up space is relevant to problems of fluid flows in heat exchangers. Flows of multi-component fluids, which components possess different properties (viscosities), have many peculiarities. In frontal displacement of a more dense and viscous fluid by a less dense and viscous one the Rayleigh-Taylor or Saffman-Taylor instability of the interface could bring to formation and growth of "fingers" of low viscosity component penetrating the bulk fluid.

The problem is also relevant to a hydrocarbon recovery. Entrapment of high viscosity fluid by the low viscosity fluid flow lowers down the quality of a hydrocarbon recovery leaving the most of viscous fluid entrapped thus decreasing the production rate.

The developed models and obtained results are applicable to description of liquid non-aqueous phase contaminants underground migration, their entrapment in the zones of inhomogenity, and forecasting the results of remediatory activities in the vicinities of waste storages and contaminated sites. Numerical investigations of the instability in displacement of viscous fluid by a less viscous one in a two-dimensional and three-dimensional geometry were carried out and analyzed before. [1-8, 15-17].

However, an important problem is flushing out of viscous fluid entrapped in porous medium. The problem is relevant to underground removal of liquid contaminants and to secondary extraction of entrapped oil from host rock formations. The present paper provides an approach to investigating this problem and developing optimal strategies for flushing out entrapped viscous fluid from porous media.

2 Experiments on fluid displacement in a Hele-Shaw cell

Peculiarities of fluid flows in blocked up space could be much better understood in microgravity studies eliminating the masking effects of thermogravitational convection, density difference, etc., and permitting to concentrate attention on multi-component convection only.

The microgravity experiments were performed in the framework of the 25th ESA parabolic flight campaign of the Airbus A300 Zero-G and are described in[13, 14].

The Hele-Shaw cell provides a gep of variable width. It was built of two plates of 10 mm thick Lexan glass that were 150x200 mm^2. They were separated by a spacer that is 25 mm wide and closes three sides of the cell. Two spacers of different width were used in order to vary the cell width δ, namely 1.2 and 3.7 mm. Rubber sheets were placed on both sides of the spacer for leakproofness. All together was fixed with screws spaced every 25 mm along the edges. The injection side was screwed on a slot valve and was proof thanks to an o-ring pressed around the injection slot. This latter was 100 mm large and 4 mm high. The inlet was then planar on the contrary of the outlet that was a 5 mm diameter hole in the bottom of lexan plate. In order to prevent the influence of the outlet geometry on the linear streamlines, cavities were drilled on all the width in the lexan plate, perpendicularly, just before the outlet.

Some examples of injection phase performed under microgravity conditions are shown in Figure 1. The liquid was injected uniformly into the cell by the slot valve. It displaced the steady pre-filling fluid of water-glycerine solution.

The characteristic dimensions of the fluid filled domain $L \times H \times \delta$ were: length L=200 mm, width H=100 mm. Thickness δ varied in different experiments. Besides mean flow velocity $U = \frac{Q}{H\delta}$ and viscosity ratio $M = \frac{\mu_2}{\mu_1}$ were also varied in experiments. Table 1 gives the description of experiments, which results are illustrated in Figure 1 in the form of two successive pictures of the displacement front for times t_1 and t_2 for each experiment.

	M	U, $\frac{sm}{s}$	d, mm	t_1, s	t_2, s
1	84	5	1.2	0.4	1.6
2	9	5	1.2	0.4	1.6
3	84	1	3.7	2	8
4	9	1	3.7	2	8

Table 1.

The succession of images in Figure 1 corresponds to their numbers in the Table 1.

The results of experiments show, that all the parameters under investigation produce an effect on the displacement process. For high viscosity ratio fingers have pear-shaped form with the heads separating and continuing independent motion as blobs of less viscous fluid moving through a more viscous one. Such separated blobs are clearly seen in Figure 1. This is in a good coincidence with our numerical results, which showed that the head of a pear-shaped finger separates and moves independently advancing in a more viscous fluid under the influence of the imposed pressure gradient [13, 16].

The instability in displacement of a viscous fluid by a less viscous one brings to the formation of a mixing zone.

3 Mathematical model

In the dimensionless form, it is reduced to the following system of equations, boundary and initial conditions:

$$\frac{\partial \mu(s)}{\partial x}\frac{\partial \psi}{\partial x} + \frac{\partial \mu(s)}{\partial y}\frac{\partial \psi}{\partial y} = 0, \tag{1}$$

$$u = \frac{\partial \psi}{\partial y}, \quad v = -\frac{\partial \psi}{\partial x}, \tag{2}$$

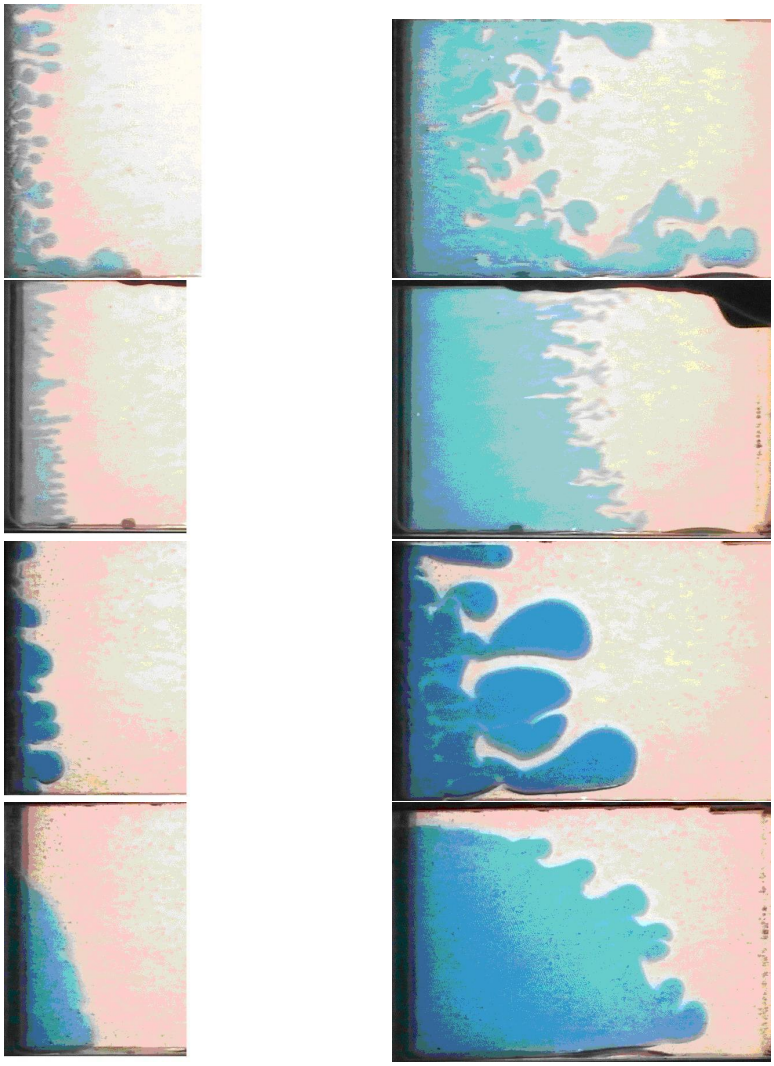

Figure 1: The succession of flow images for different cases of displacement of a viscous fluid by a less viscous one. The experimental conditions are provided in Table 1.

$$\frac{\partial s}{\partial t} + \frac{\partial (us)}{\partial x} + \frac{\partial (vs)}{\partial y} = \frac{\partial^2 s}{\partial x^2} + \frac{\partial^2 s}{\partial y^2}, \tag{3}$$

$$\mu(s) = M^{-s}, \tag{4}$$

$$x = 0, x = A \cdot Pe, y = \pm\frac{Pe}{2}: \quad \psi = y, \tag{5}$$

$$x = 0, x = A \cdot Pe, s = 1: \quad \frac{\partial s}{\partial x} = 0, \tag{6}$$

$$y = \pm\frac{Pe}{2}: \quad \frac{\partial s}{\partial x} = 0, \tag{7}$$

$$t = 0: \quad s = 0. \tag{8}$$

The equation (1) is related to distribution of the stream function ψ; it is derived from the Darcy law, the incompressibility and the absence of gravity force conditions. The expressions (2) are related to definition of the stream function. The equation (3) states for the intruding fluid saturation dynamics. The expression (4) determines dimensionless fluid viscosity depending on saturation (more saturation, less viscosity; the type of dependence

generalizes harmonic averaging). The boundary conditions (5) state for solidity of lateral walls at $y = \pm\frac{Pe}{2}$ and regularity of intruding fluid flow at the inlet ($x = 0$) and outlet ($x = A \cdot Pe$) boundaries. The boundary conditions (6), (7) state for the inflow of the intruding fluid only, free outflow of the mixture, von Neumann's conditions for the saturation affected by diffusion on the lateral walls. The initial condition (8) says that the domain is not filled with the intruding fluid at the first instance. The co-ordinate system origin is placed in the middle of the inlet section.

The equation (1), expression (2) and boundary conditions (5) were derived from the continuity equation, Darcy law and the non-permeability of lateral walls, correspondingly:

$$\frac{\partial u}{\partial x} + \frac{\partial v}{\partial y} = 0, \tag{9}$$

$$u = -\mu^{-1}\frac{\partial p}{\partial x}, \quad v = -\mu^{-1}\frac{\partial p}{\partial y}, \tag{10}$$

$$y = \pm\frac{Pe}{2}: \quad v = 0. \tag{11}$$

The dimensionless parameters in the relationships (1)-(7) are determined as follows:

$$A = \frac{L}{H}, \quad M = \frac{\mu_2}{\mu_1}, \quad Pe = \frac{Q}{D} = \frac{UH}{D}, \tag{12}$$

where L, H are the length and the width of the domain, μ_1, μ_2 are viscosity of intruding and displaced fluids, respectively, Q is the amount of intruding fluid per time unit, U is the average velocity of insertion.

The following scaling factors are used to derive dimensional values from dimensionless ones:

$$\bar{u} = U \cdot u, \bar{v} = U \cdot v, \bar{x} = \frac{D}{U} \cdot x, \bar{y} = \frac{D}{U} \cdot y, \bar{t} = \frac{D}{U^2} \cdot t, \bar{\psi} = D \cdot \psi. \tag{13}$$

Here, values with a bar denote the dimensional parameters relating to dimensionless ones without the bar over them.

Dimensionless viscosity μ is proportional to the dimensional one $\bar{\mu}$ and is scaled upon the viscosity of the fluid being displaced and permeability K of the porous skeleton:

$$\bar{\mu} = \frac{K}{\mu_2} \cdot \mu. \tag{14}$$

4 Numerical simulations

Numerical simulations were performed in a 2-D domain having original size $200mm \times 100mm$, which corresponds to the experimental cell described above. Numerical modeling was performed for the case of a homogeneously permeable medium, which corresponds to a Hele-Shaw cell with flat parallel walls, and for the cases of inhomogeneous permeability as well, which corresponds to the case of obstacle placing in the gap between the two walls in the Hele-Shaw cell.

We used Eulerian approach to solve the problem stated above; the rectangular grid with uniform space steps was involved. Using CFL (Courant - Friedrichs - Levi) criterion we determined the next time step value [9]. Using 2D TVD (2-dimensional total variation diminishing) techniques of the second order [10] we transferred the hyperbolic part of the concentration equation (3) to the next time layer. Using 2D Buleev technique (implicit iterative method for elliptic equations using incomplete factorisation [11] we transfer the parabolic part of the concentration equation (3) to the next time layer.

5 Frontal displacement

Numerical modeling of displacement for fluids of equal viscosity was carried out to validate the scheme. The results shown in Figure 2 testify, that the displacement is stable for the viscosity ratio M=1. Numerical scheme under consideration does not introduce any instability.

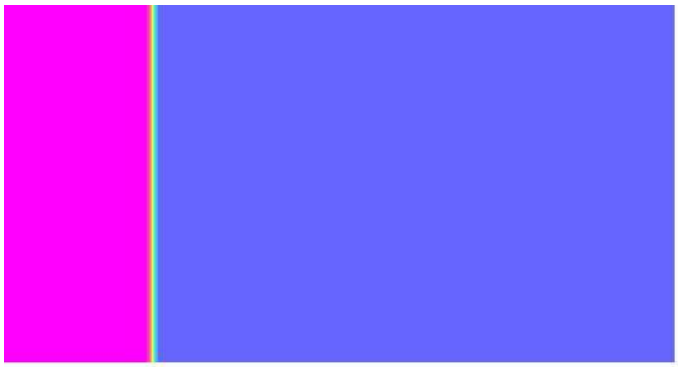

Figure 2: Saturation maps for viscous fluids displacement: viscosity ratio M=1, dimensionless time $\tau = \frac{tV}{L} = 0.219$.

As it is known, the increase of viscosity ratio for the displaced and displacing fluids promotes instability in frontal displacement from a homogeneous medium. Figure 3 illustrates the saturation map for the case of high viscosity ratio M=84.

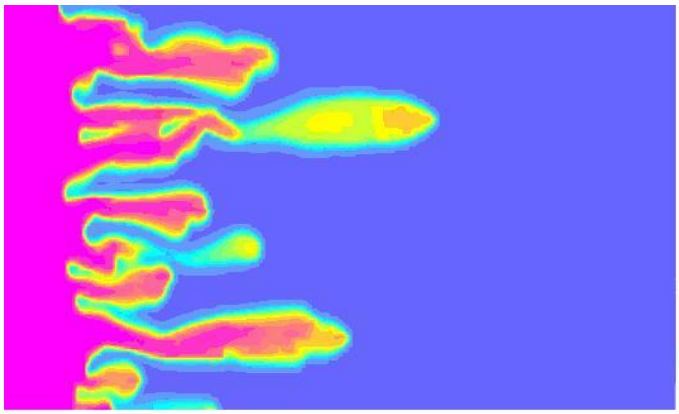

Figure 3: Saturation maps for viscous fluids displacement: viscosity ratio M=84, dimensionless time $\tau = \frac{tV}{L} = 0.248$.

The results show, that the interface instability arising in viscous fluids displacement (for $M > 1$) brings to formation of fingers of less viscous fluid penetrating the more viscous one. Those fingers grow in time. Some of fingers have the tendency to acquire a peer-shape with the neck getting thinner, and then separate from the displacing fluid. Those separated blobs of less viscous fluid move independently through the more viscous one under the influence of imposed pressure gradient as if floating up in the gravity field. In time mixing of low viscosity fluid with the surrounding one takes place due to diffusion, and the blobs slow down to the velocity of the flow. The traces of the separated blobs,

which diffused before, serve as a preferable pathway for new fingers to develop. This type of displacement instability was studied in details in [16, 17].

6 Flushing out entrapped viscous fluid by a more viscous one

Numerical simulation of the process were undertaken for different values of dimensionless governing parameters. The two-dimensional domain under investigation in the initial state looked as shown in Figure 4. The entrapped less viscous fluid occupied a cylindrical domain. Both fluids were assumed Newtonian. Figures 5-8 illustrate concentration maps for successive stages of entrapped fluid flushing out.

Figure 4: Entrapped viscous fluid concentration in a porous specimen.

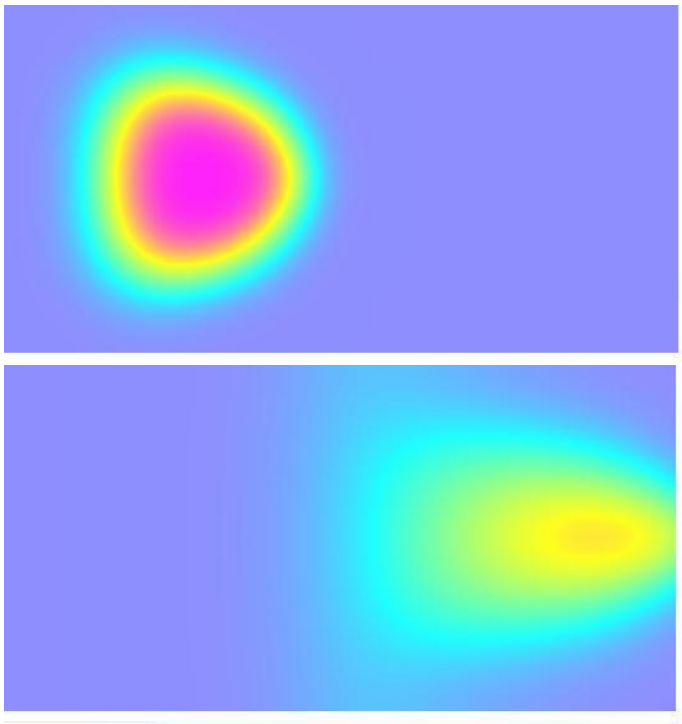

Figure 5: Successive stages of flushing out process. Viscosity ratio M=10,Peclet number Pe=100.

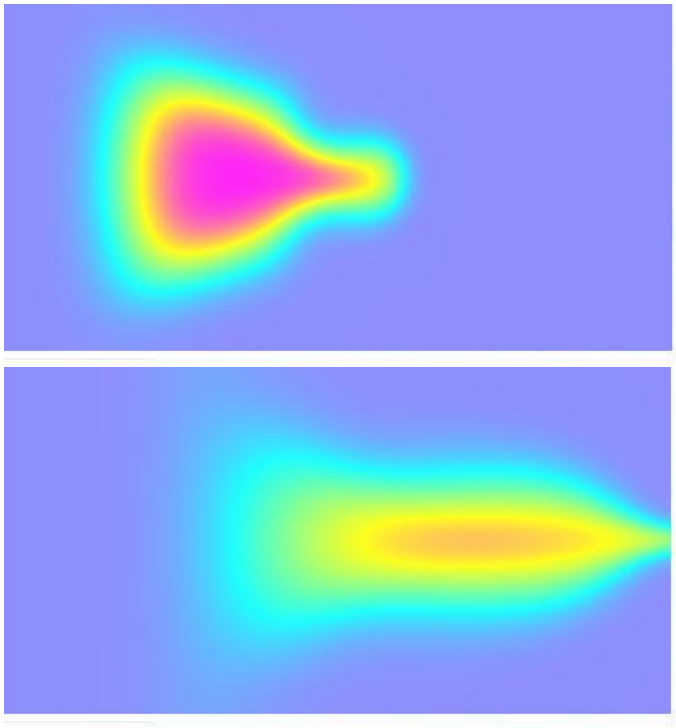

Figure 6: Successive stages of flushing out process. Viscosity ratio M=1000, Peclet number Pe=100.

7 Flushing out entrapped viscous fluid by a less viscous one

The next series of numerical experiments was performed for the case of flushing out of more viscous fluid by a less viscous one. In order to follow the process the computational domain was longer, thus the aspect ratio does not match that in experiments. The results are shown below. The calculations were performed for the following values of governing parameters:

$A = 0.2 = \frac{H}{L}$, where L, H are the length and the width of the domain,

$X_c = 0.1$ - initial co-ordinate of the center of the "droplet",

$R_c = 0.05$ - "droplet" initial radius.

Figure 9 illustrates the successive stages of displacement process for the case $M = \frac{\mu_2}{\mu_1} = 0.3, Pe = 5000$. Line segments in the figure correspond to directions of fluid velocity their length being proportional to velocity modulus.

The results show that for this case instability arises in the front boundary of the droplet. Comparison of two different scenarios: flushing out by less viscous fluid, and by a more viscous fluid, shows that in all cases interface instability arises at interfaces, on which fluid viscosity growth direction coinsides with direction of the overall flow. These qualitative results obtained in numerical simulations were first published in [14] Comparison of present numerical simulations of flushing out entrapped fluid from a thin gap with experimental results illustrated in [20] testifies good agreement.

In case Peclet number is smaller, manifestation of front interface instability is not so evident. However, the tendency of zone separation is still present. Figure 10 illustrates the successive stages of displacement process for the case $M = \frac{\mu_2}{\mu_1} = 0.1, Pe = 100$.

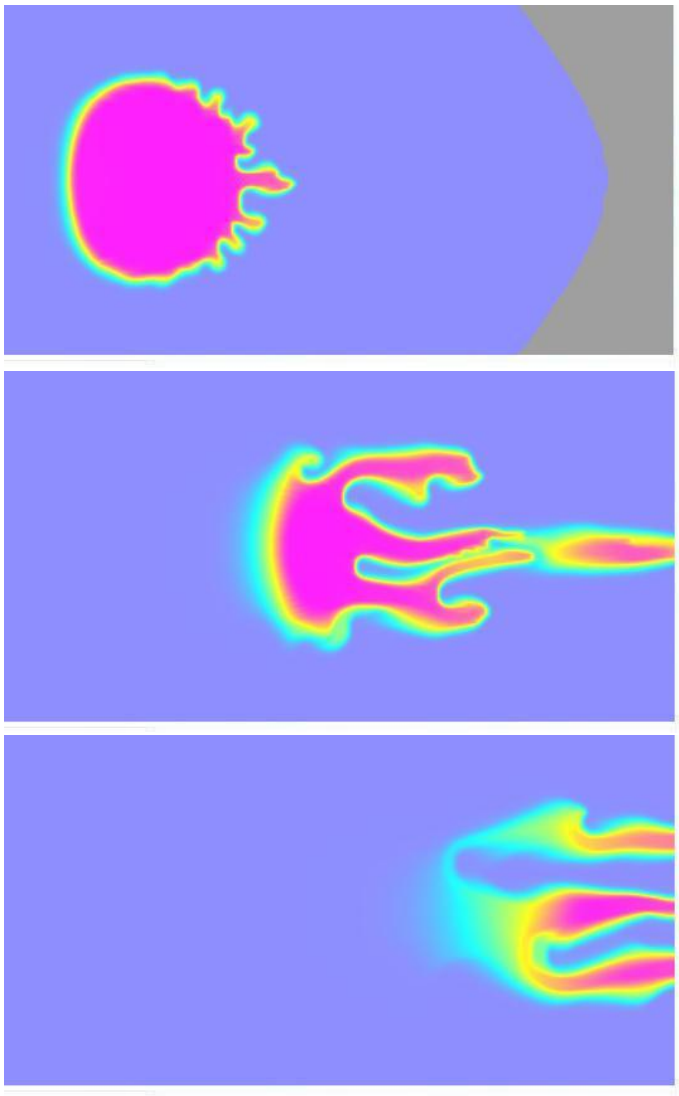

Figure 7: Successive stages of flushing out process. Viscosity ratio M=10, Peclet number Pe=10000.

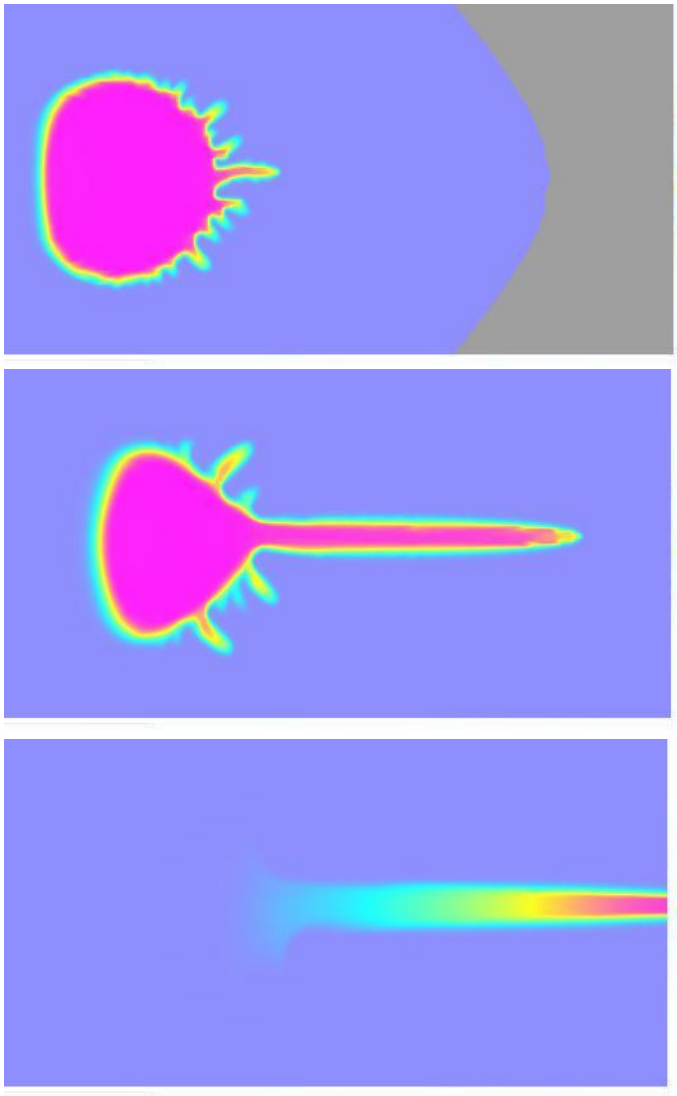

Figure 8: Successive stages of flushing out process. Viscosity ratio M=1000, Peclet number Pe=10000.

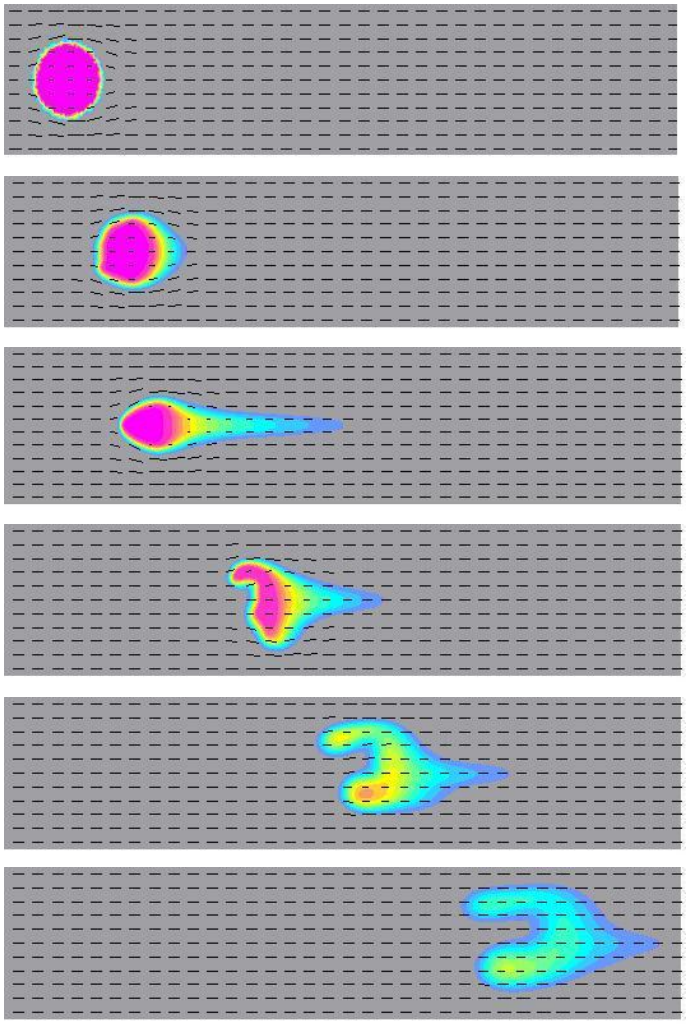

Figure 9: Entrapped fluid concentration maps for successive stages of flushing out more viscous fluid by a less viscous one. Viscosity ratio M=0.3, Peclet number Pe=5000.

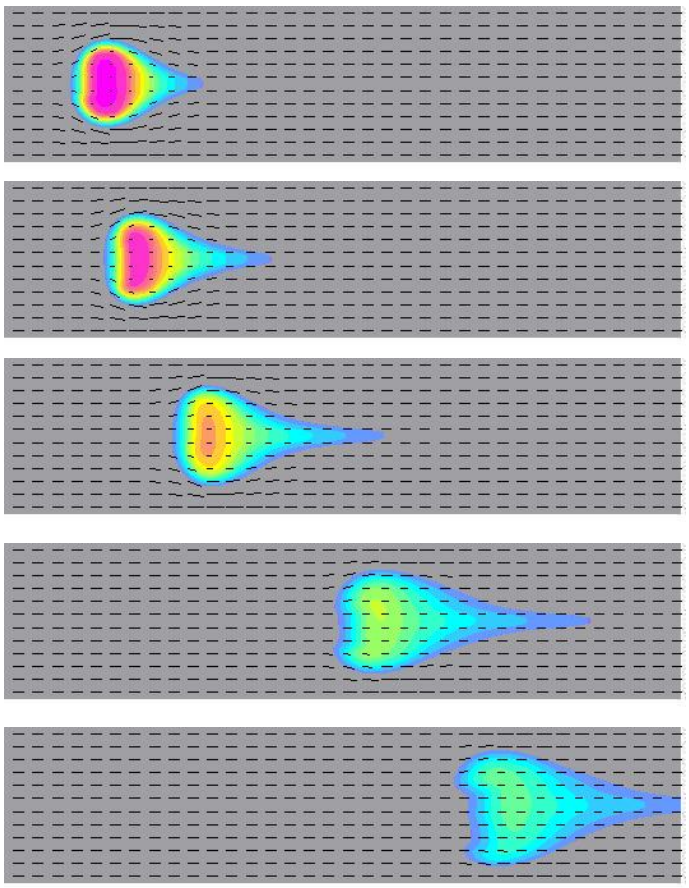

Figure 10: Entrapped fluid concentration maps for successive stages of flushing out more viscous fluid by a less viscous one. Viscosity ratio M=0.1, Peclet number Pe=100.

8 Conclusions

- Comparison of experimental results on displacement with that of numerical modeling demonstrated a good coincidence and testified the adequacy of the developed mathematical model.
- Experimental and numerical investigations showed that some fingers had the tendency to acquire a peer-shape with the neck getting thinner, and then separate from the displacing fluid.
- In displacement of an entrapped viscous fluid by a streaming flow of a more viscous one originating fingers are located on the rear part of the entrapped less viscous body. The increase of Peclet number and viscosity ratio brings to the increase of the number of fingers. However, the growth of the axial one is predominant.
- In displacement of an entrapped viscous fluid by a streaming flow of a less viscous one originating fingers are located on the front part of the entrapped less viscous body forming, sometimes, peculiar patterns and separating the initially entrapped compact body into several pieces.

Acknowledgements

The authors wish to acknowledge the generous support of Russian Foundation for Basic Research (RFBR Project 12-08-00198).

References

[1] Barenblatt G.I., Entov V.M., Ryzhik V.M. Theory of fluids flows through natural rocks. Kluwer Academic Publishers - Dordrecht / Boston / London, 1990.

[2] V.R. Dushin, V.F. Nikitin, J.C. Legros, M. Thiercelin. Seepage flows instability in porous media. Acta Astronautica, 2009, vol. 64, pp. 295-312.

[3] Bear J., Bachmat Y. Introduction to modelling of transport phenomena in porous media. Kluwer Academic Publishers-Dordrecht/Boston/London, 1990.

[4] Kaviany M. Principles of heat transfer in porous media. Dover Publications Inc. - New York, 1988.

[5] Smirnov N.N., Dushin V.R., Legros J.C., Istasse E., Bosseret N., Mincke J.C., Goodman S. Multiphase flow in porous media - mathematical model and micro-gravity experiments. Microgravity Science and Technology, IX(3), 1996, pp. 222-231.

[6] Smirnov N.N., Legros J.C., Nikitin V.F., Istasse E., Norkin A.V., Shevtsova V.M., Kudryavtseva O.V. Capillary driven filtration in porous media. . Microgravity Science and Technology, Hanser Publ., 1999, XII, pp. 23-35.

[7] Smirnov N.N., Nikitin V.F., Norkin A.V., Kiselev A.B., Legros J.C., Istasse E. Microgravity investigation of capillary forces in porous media. Space Forum 2000, 6(1-4), pp. 1-10.

[8] De Wit A., Homsy G.M. Viscous fingering in periodically heterogeneous porous media. Part II. Numerical simulations. J. Chem. Phys. 1997. Vol. 107(22), 9619.

[9] Anderson D.A., Tannenhill J.C., Pletcher R.H. Computational fluid mechanics and heat transfer. New York, McGraw-Hill, 1984.

[10] Yee H.C., Warming R.F., Harten A. Implicit total variation diminishing (TVD) schemes for steady-state calculations. Journal of Computational Physics, 57, pp. 327-360 (1985).

[11] Ilyin V.P. Incomplete factorisation methods for solving algebraic systems. Moscow, Nauka publishes, 1995 (in Russian).

[12] Nikitin V.F., Smirnov N.N., Legros J.C. Effect of fingering in porous media. 52-d IAF Congress. Toulouse, 2001, IAF-01-J.4.10.

[13] Smirnov N.N., Nikitin V.F., Ivashnyov O.E., Maximenko A., Thiercelin M., Vedernikov A., Scheid B., Legros J.C. Microgravity investigations of instability and mixing flux in frontal displacement of fluids. Microgravity sci. technol. 2004, XV/3, pp. 3-28.

[14] Dushin V.R., Nikitin V.F., Phylippov Yu.G., Legros J.C. Two-component fluidconvective flow in thin gaps. Acta Astronautica, 2010, vol. 66, 742-747.

[15] Smirnov N.N., J. C. Legros, V. F. Nikitin, E. Istasse, L. Schramm, F. Wassmuth, and D'Arcy Hart. Filtration in Artificial Porous Media and Natural Sands under Microgravity Conditions. Microgravity sci. technol. 2003, XIV/2, pp. 3-28.

[16] Smirnov N.N., Nikitin V.F., Maximenko A., Thiercelin M., Legros J.C. Instability and mixing flux in frontal displacement of viscous fluids from porous media. Physics of Fluids, 2005, vol.17, 084102.

[17] Smirnov N.N., Nikitin V.F., Dushin V.R., Maximenko A., Thiercelin M., Legros J.C. Instability in displacement of viscous fluids from porous specimens, Acta Astronautica, 2007, vol. 61, No 7-8, pp. 637-643.

[18] Smirnov N.N., Kisselev A.B, Nikitin V.F., Zvyaguin A.V., Thiercelin M., Legros J.-C. Hydraulic filtration and fracturing in porous medium. Proc. 2nd Internat. Conf. on Thermal Engineering. Al Ain, UAE. 2006. p. 683-690.

[19] Dushin, V.R., Nikitin, V.F., Philippov, Yu.G., Smirnov, N.N. Two phase flows in porous media under microgravity conditions Microgravity Science and Technology 2008, vol. 20 (3-4), pp. 155-160.

[20] R. Maes, G. Rousseaux, B. Scheid, M. Mishra, P. Colinet, A. De Wit. Experimental study of dispersion and miscible viscous fingering of initially circular samples in Hele-Shaw cells. Physics of Fluids, 2010, vol. 22, 123104.

N. N. Smirnov, V. F. Nikitin, Yu. G. Phylippov, V. R. Dushin, Moscow M.V. Lomonosov State University, Moscow, Russia

N. N. Smirnov, V. F. Nikitin, V. R. Dushin, Scientific Research Institute for System Analysis of the Russian Academy of Sciences, Moscow, Russia